TURBULENT DISPERSION IN THE ATMOSPHERIC SURFACE LAYER

J. D. WILSON*

Atmospheric Environment Service, 4905 Dufferin St., Downsview, Ontario, Canada

Abstract. By non-dimensionalizing a trajectory-simulation (TS) model of turbulent dispersion, it is shown that the dimensionless concentration $z_0 c u_*/kQ$ (cu_*/kQ) due to a continuous line (area) source of strength Q in the atmospheric surface layer depends only on z/z_0, x/z_0, z_0/L and z_s/z_0, where z_s is the source height. The TS model is used to tabulate concentration profiles due to ground-level line and area sources. Concentration profiles generated by the TS model for elevated sources are shown to be inconsistent with the Reciprocal Theorems of Smith (1957) and it is suggested that this is because the flux-mean gradient closure scheme inherent in the Reciprocal Theorem is invalid for an elevated source.

1. Introduction

This paper is concerned with short-range dispersion of a passive admixture from a continuous line or plane (area) source in the horizontally homogeneous atmospheric surface layer. Wilson *et al.* (1981a, b, c) have described a method of simulation of particle trajectories in inhomogeneous turbulence which leads to predictions in precise agreement with analytical solutions where available, and in good agreement with atmospheric observations. It will be shown here that the trajectory-simulation (TS) model predicts that the dimensionless concentration $\chi = z_0 c u_*/kQ$ downwind of a line source is a function only of z/z_0, x/z_0, z_0/L, and z_s/z_0, where z_0 is the roughness length, $c(x, z)$ the concentration, u_* the friction velocity, k von Karman's constant (0.4 used herein), Q the source strength, x the fetch, L the Monin-Obukhov length (defined later) and z_s the source height. This scaling is in agreement with predictions obtained by the application of the Lagrangian Similarity Hypothesis to turbulent dispersion (see Cermak, 1962) and by numerical integration of the diffusion equation (Yamamoto and Shimanuki, 1961).

The equations underlying the TS model are briefly reviewed and then non-dimensionalised. It is shown that the concentration profiles predicted by the model do not obey the Reciprocal Theorem which relates the profile due to an elevated source to the profile due to a ground-level source. Predictions of the model for dispersion from ground-level line and plane sources are tabulated for a useful range of values of the fetch x/z_0 and stability z_0/L.

2. Review of the Trajectory-Simulation Model

Consider a two-dimensional horizontally homogeneous surface layer in which the Eulerian horizontal (x) velocity u is steady and depends only on the height (z) and in

---

* Present affiliation: New Zealand Meteorological Service, P.O. Box 722, Wellington, New Zealand.

which the Eulerian vertical velocity w is unsteady (turbulent) with a time average value of zero. The Eulerian velocity, time, and length scales are:

$$\sigma_w(z) = (\overline{w^2})^{1/2}$$

$$\tau(z) = \int_0^\infty \overline{w(z, t)\, w(z, t + T)}\; \mathrm{d}T / \sigma_w^2$$

$$\Lambda(z) = \sigma_w(z)\, \tau(z)$$

where the overbar denotes a time average.

Wilson et al. (1981a, b) have shown that each step in a fluid element trajectory in such a system may be calculated using:

$$\Delta z = [w_L(t_H) + w_*]\; \frac{\sigma_w(z)\, \tau_L(z)}{\sigma_w(H)\, \tau_L(H)}\; \Delta t_H \tag{1a}$$

$$= \frac{\Lambda_L(z)}{\Lambda_L(H)}\; \Delta z_*$$

$$\Delta z_* = (w_L(t_H) + w_*)\Delta t_H \tag{1b}$$

$$\Delta x = u(z)\; \frac{\tau_L(z)}{\tau_L(H)}\; \Delta t_H. \tag{1c}$$

Here τ_L is the Lagrangian time scale, a measure of the persistence of the vertical velocity of a marked fluid element, and it is assumed that $\tau_L(z) \alpha \tau(z)$. The Lagrangian velocity scale is assumed to be equal to the Eulerian velocity scale, so that the Lagrangian length scale $\Lambda_L = \sigma_w \tau_L$ is proportional to the Eulerian length scale.

The height H is a reference height, and a subscript H implies a value at $z = H$. The choice of H is completely arbitrary. t_H is a transformed time, related to real time t by:

$$\frac{\mathrm{d}t}{\tau_L(z)} = \frac{\mathrm{d}t_H}{\tau_L(H)}$$

and the timestep Δt_H is chosen as $\Delta t_H \lesssim \tau_L(H)/10$.

z_* is a transformed height axis, and the fluid element trajectories are calculated in the (x, z_*, t_H) system in which the scales of the turbulent motion are independent of position. The fluctuating Lagrangian velocity $w_L(t_H)$ is a record of vertical velocity appropriate to a fluid element moving at the reference height H, having timescale $\tau_L(H)$ and velocity scale $\sigma_w(H)$. This may be generated using a Markov chain

$$w_L(t_H + \Delta t_H) = w_L(t_H) \exp\left(-\Delta t_H / \tau_L(H)\right) +$$
$$+ \left(1 - \exp\left(-2\Delta t_H / \tau_L(H)\right)\right)^{1/2} \sigma_w(H) r$$

where r is chosen at random from a normal distribution with mean zero and variance 1.

w_* is a bias velocity, necessary to incorporate the effect of variation of σ_w with height, and is given by $w_* = \sigma_w(H)\tau_L(z)\,d\sigma_w/dz$. The equivalent velocity along the z-axis is $\Lambda_L(z)\,d\sigma_w/dz$.

Equations (1) are compatible with Batchelor's (1957) hypothesis of Lagrangian similarity: while the Lagrangian vertical velocity of a fluid element moving along the z-axis is not a stationary function of time, $w_L(t_H)$ is a stationary random function of transformed time t_H.

Equations (1) were used by Wilson $et\ al.$ (1981c) to simulate motion in the atmospheric surface layer. The height dependence of the Lagrangian timescale $\tau_L(z)$ was determined by a comparison of model predictions with the Project Prairie Grass data set. With a suitable choice for $\tau_L(z)$, there was excellent agreement between the predictions of the TS model and the experimental data over a wide range of values of the Monin-Obukhov length.

3. A Non-dimensional Form for the Trajectory-Simulation Model

In this section it will be shown that the trajectory-simulation model may be formulated in terms of non-dimensional variables to eliminate the need for specification of z_0. To simplify the notation, the subscript L is dropped; all variables are Lagrangian unless otherwise specified. A subscript N denotes the value of a property under neutral stratification and a subscript H the value at $z = H$.

The following symbols are used: $\eta = z/z_0$, dimensionless height; $\lambda = z_*/\Lambda_N(H)$, dimensionless height on z_* axis, where $\Lambda_N(H) = 0.5H$; $\xi = x/z_0$, dimensionless downwind distance; $\Omega = z_0/L$, dimensionless stability parameter; $\mathscr{L} = \Lambda(z)/z_0$, dimensionless length scale.

z_0 appears in Equations (1) through $u(z)$, which is obtained by integrating the expression:

$$\frac{kz}{u_*}\frac{du}{dz} = \phi_m\left(\frac{z}{L}\right)$$

subject to the condition that $u(z_0) = 0$. Here L is the Monin-Obukhov length,

$$L = -u_*^3 \bigg/ \left(k\,\frac{g}{T_0}\,\frac{A}{\rho c_p}\right),$$

ϕ_m is the Monin-Obukhov universal function for momentum, g is the gravitational acceleration, T_0 is a reference temperature, A is the sensible heat flux density (positive in unstable stratification), ρ is the density of the air, and c_p is the specific heat at constant pressure. ϕ_m is given by:

$$\phi_m = \begin{cases} 1 & L = \infty \\ 1 + \beta_u^+\, z/L & L > 0 \\ (1 + \beta_u^-\, z/L)^{-1/4} & L < 0 \end{cases}$$

where $\beta_u^+ \simeq 4.7$ and $\beta_u^- \simeq -16$ (Haugen, 1973). The wind profile, expressed as a function of the non-dimensional variables, is:

$$u(\eta, \Omega, u_*) = \frac{u_*}{k} \times \begin{cases} \ln \eta & L = \infty \\ \ln \eta + \beta_u^+ \Omega(\eta - 1) & L > 0 \\ 2 \arctan \phi_m^{-1} + \ln \dfrac{\phi_m^{-1} - 1}{\phi_m^{-1} + 1} - k_u & L < 0 \end{cases}$$

$$= \frac{u_*}{k} \, U(\eta, \Omega)$$

where

$$k_u = 2 \arctan \phi_{m0}^{-1} + \ln \frac{\phi_{m0}^{-1} - 1}{\phi_{m0}^{-1} + 1}$$

and $\phi_{m0}^{-1} = (1 + \beta_u^- \Omega)^{1/4}$.

The velocity scale in the surface layer obeys:

$$\sigma_w(\eta, \Omega, u_*) = bu_* G(\eta, \Omega)$$

where

$$G(\eta, \Omega) = \begin{cases} 1 & L > 0, \quad L = \infty \\ (1 + \beta_w \Omega \eta)^{1/3} & L < 0 \end{cases}$$

$b \simeq 1.25$ and $\beta_w \simeq -4.1$.

The dimensionless length scale $\mathscr{L}$ which follows from the recommendations of Wilson *et al.* (1981c) is:

$$\mathscr{L}(\eta, \Omega) = a\eta \times \begin{cases} 1 & L = \infty \\ (1 + \beta_l^+ \Omega \eta)^{-1} & L > 0 \\ (1 + \beta_l^- \Omega \eta)^{1/4} & L < 0 \end{cases}$$

with $a \simeq 0.5$, $\beta_l^+ \simeq 5$ and $\beta_l^- \simeq -6$.

The vertical step may be written:

$$\Delta z = (w_{HN} + \hat{w}_*) \frac{\Lambda(z)}{\Lambda_N(H)} \Delta t_{HN}. \tag{1'a}$$

Note that this differs from the vertical step of Equation (1a) in that the velocity record at H always has scales $\sigma_{wN}(H)$ and $\tau_N(H)$. However these values of the time and velocity scales transform to give the correct (height and stability-dependent) scales in the z-system. The bias velocity is:

$$\hat{w}_*(\eta, \Omega, u_*) = \sigma_{wN}(H)\, \tau(z)\, d\sigma_w/dz$$

$$= \sigma_{wN}(H)\, \mathscr{L}(\eta, \Omega)\, \frac{d \ln G(\eta, \Omega)}{d\eta}\,.$$

The corresponding horizontal step is:

$$\Delta x = u(z)\, \frac{\tau(z)}{\tau_N(H)}\, \Delta t_{HN} = u(z)\, \frac{\Lambda(z)}{\sigma_w(z)\, \tau_N(H)}\, \Delta t_{HN} \tag{1'c}$$

where u is the stability-corrected windspeed.

The non-dimensional forms of the distance steps are:

$$\Delta \eta = (w_{HN} + \hat{w}_*)\, \frac{\mathscr{L}(\eta, \Omega)}{\Lambda_N(H)}\, \Delta t_{HN}$$

$$= \mathscr{L}(\eta, \Omega)\Delta\lambda \tag{2a}$$

$$\Delta\lambda = (w_{HN} + \hat{w}_*)\Delta t_{HN}/\Lambda_N(H) = \gamma(w_{HN} + \hat{w}_*)/\sigma_{wN}(H) \tag{2b}$$

$$\Delta\xi = \gamma U(\eta, \Omega)\mathscr{L}(\eta, \Omega)/(kbG(\eta, \Omega)) \tag{2c}$$

where $\gamma = \Delta t_{HN}/\tau_N(H) \simeq 0.1$. Note that $\Delta\lambda$ and $\Delta\xi$ are independent of u_* and z_0.

Corresponding to Equation (2a), which relates the height-increments on the η and λ axes, there is the relationship $d\eta = \mathscr{L}(\eta, \Omega)\, d\lambda$ which relates the η and λ coordinate axes. The latter may be integrated to obtain

$$\lambda/2 = z_*/H = \begin{cases} \ln \eta & L = \infty \\[2mm] \ln \eta + \beta_l^+ \Omega(\eta - 1) & L > 0 \\[2mm] 2 \arctan f + \ln \dfrac{f - 1}{f + 1} - k_l & L < 0 \end{cases} \tag{3}$$

where

$$f = (1 + \beta_l^- \Omega\eta)^{1/4}$$

$$k_l = 2 \arctan f_0 + \ln \frac{f_0 - 1}{f_0 + 1}$$

$$f_0 = (1 + \beta_l^- \Omega)^{1/4}\,.$$

The integration constant has been determined by specifying that $\eta = 1$ at $\lambda = 0$. This implies that trajectories are reflected at $z = z_0$.

Because of the (known) relationship between η and λ, the functional dependence of U, G, $\hat{w}_*$, $\mathscr{L}$ on η may be replaced with a functional dependence on λ. The trajectory may then be calculated in (λ, ξ, t_{NH}) coordinates.

The λ axis is divided into layers of depths $\delta\lambda$ labelled by $\lambda(I) = (I - 0.5)\delta\lambda$. $\delta\lambda$ is chosen to be of the order of the typical step length, $\delta\lambda \sim \gamma \sim 0.1$. To each $\lambda(I)$ there corresponds $\eta(I)$ which is determined by solving Equation (3); in non-neutral stratification this requires the use of Newton's Method of Successive Approximations (Abramowitz and Stegun, 1970) because Equation (3) is implicit in η. Having determined the $\eta(I)$, the values of $\Delta\xi$ and $\hat{w}_*$ at each $\lambda(I)$ are tabulated. The trajectories are then calculated in steps:

$$\Delta\lambda = \gamma(w_{HN} + \hat{w}_*)/\sigma_{wN}(H)$$

$$\Delta\xi = \Delta\xi(\lambda)$$

where w_{HN} is formed from the Markov chain.

The chosen values of $I^{\max}$ (maximum number of layers) and $\delta\lambda$ must ensure that the values of $\Delta\xi$ and $\hat{w}_*$ are tabulated out to a height $(z/z_0)^{\max}$ above which very few particles climb in the chosen fetch. It was usually ensured that $(z/z_0)^{\max} \sim x/z_0$.

If NP particles are released at $x = 0$ and a counter $N(I)$ is incremented each time a particle passes the collector at $x = X$ in layer I, then the real-world time average horizontal flux at dimensionless height $\eta(I)$ is predicted to be

$$F_x(I) = \frac{QN(I)/\text{NP}}{\delta z(I)} \tag{4}$$

and the time average concentration at $\eta(I)$ is predicted to be

$$c(I) = F_x(I)/u(I) = \frac{QN(I)/\text{NP}}{u(I)\delta z(I)} \tag{5}$$

where Q is the strength of the line source [number or $g\,cm^{-1}\,s^{-1}$]. The values $N(I)$ depend on z_0 only through the ratio z_0/L. Nor do they depend on u_*: if u_* doubles then σ_w, w_{HN}, $\hat{w}_*$, and u are all doubled but $\Delta\xi$ and $\Delta\lambda$ are unchanged.

The denominator of Equations (4) and (5) contains the depth of the Ith layer,

$$\delta z(I) = z_0\,\delta\eta(I) = z_0\,\mathscr{L}(\eta(I))\,\delta\lambda\,.$$

It follows that:

$$\chi = \frac{z_0 c(I)u_*}{kQ} = \frac{N(I)/\text{NP}}{U(\eta(I))\mathscr{L}(\eta(I))\delta\lambda}\,.$$

The dimensionless concentration χ depends on z_0 only through z_0/L and is independent of u_*, i.e., $\chi = \chi(z/z_0, x/z_0, z_0/L, z_s/z_0)$. Similarly in the case of an area source of strength Q [number or $g\,cm^{-2}\,s^{-1}$] it may be shown that the dimensionless concentration cu_*/kQ has dependence only on z/z_0, x/z_0, z_0/L, z_s/z_0.

That χ depends on z_0 only through z_0/L has interesting implications for practical air pollution assessment schemes. For example, according to the Gaussian Plume model, the ground-level concentration due to a line source at $z = z_s$ a distance x upstream is:

$$c_0(x, z_0, z_s, L, u_1) = \sqrt{\frac{2}{\pi}} \frac{Q}{u_1 \sigma_z} \exp\left(-z_s^2/2\sigma_z^2\right)$$

where the model (being strictly applicably only to homogeneous turbulence with no wind shear) allows a single value u_1 for the windspeed and where for atmospheric applications one writes $\sigma_z = \sigma_z(x, z_0, z_s, L)$. A review of efforts to determine σ_z is given by Gifford (1976).

Multiplying by $z_0 u_*/kQ$, the dimensionless concentration is

$$\chi_0 = \sqrt{\frac{2}{\pi}} \frac{u_*}{ku_1 \sigma_\eta} \exp\left(-\eta s^2/2\sigma_\eta^2\right)$$

where $\eta s = z_s/z_0$ and $\sigma_\eta = \sigma_z/z_0$. One may write $(ku_1/u_*) = U(\eta_1, \Omega)$.

Rather than giving several curves of $\sigma_z(x)$ with z_0 as a parameter (see Figure 6 of Gifford's review paper), it is preferable to give a single curve of $\sigma_\eta(\xi)$ (for fixed ηs and Ω) with $U(\eta_1, \Omega)$ chosen at a standard dimensionless height η_1.

Although the TS model does not include any fluctuations u' in the horizontal velocity ($u' = u - \bar{u}$ where $\bar{u}$ is the time average and u the instantaneous velocity), the horizontal flux predicted by the model should closely approximate the true value because for long travel times the effect of u' tends to be averaged out. The concentration predicted by the model is $c^F = \overline{uc}/\bar{u}$, which is equal to the mean concentration $\bar{c}$ if $\overline{uc} = \bar{u}\bar{c} + \overline{u'c'} \simeq \bar{u}\bar{c}$.

The results of simulations using the non-dimensional TS model are given in the next section.

4. Predictions of the Trajectory-Simulation Model for Dispersion in the Surface Layer

4.1. ELEVATED SOURCES

Elevated industrial sources usually have z_s of the order of the surface layer depth (or larger) and occur in a situation where the surface-layer cannot be regarded as horizontally homogeneous. Elevated agricultural sources (chemical sprayers, irrigation sprinklers) usually require the inclusion of buoyancy and surface uptake. Therefore elevated sources will be treated very briefly here.

Figure 1 gives the predictions of the TS model for dispersion from an elevated line source and a line source at $z_s = z_0$ in the neutral surface layer. It can be seen that if $x/z_0 \gtrsim 10^2 z_s/z_0$, the profile for the elevated source is very similar to the profile for the source at z_0.

The Reciprocal Theorem of Smith (1957) states that 'the concentration at $\mathbf{x}'$ due a source at $\mathbf{x}''$, with the flow in the positive x direction, is equal to the concentration at $\mathbf{x}''$ due to an identical source at $\mathbf{x}'$ when the direction of the flow is reversed', where $\mathbf{x}$ is the position vector. Smith suggests that the Reciprocal Theorem be used to obtain the concentration profile for an elevated source from the profile for a ground-level source.
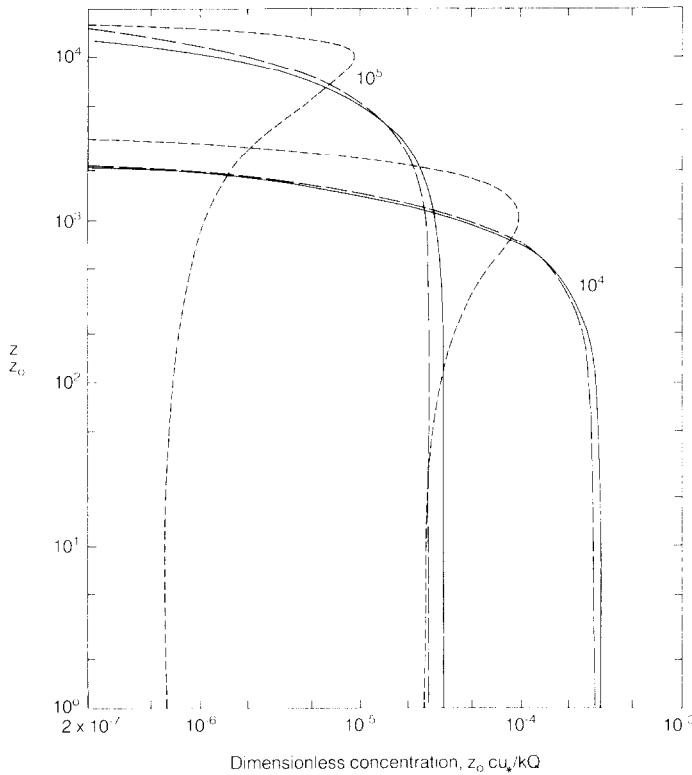
Fig. 1.   Dimensionless concentration profiles at a distance $\xi = (10^4, 10^5)$ downwind of a line source at $z_s/z_0 = 1$, (———); $z_s/z_0 = \xi/10$, (------); $z_s/z_0 = \xi/10^2$, (- - -). Neutral stratification.

As can be deduced from Figure 1, the predictions of the TS model do not obey the Reciprocal Theorem. The dimensionless concentration at $\eta = 10^3$ due to a line source at z_0 a distance $\xi = 10^4$ upstream is 4.1×10^{-5} but the ground-level value due to a line source at $\eta s = 10^3$ a distance $\xi = 10^4$ upstream is 2.75×10^{-5}, whereas according to the Reciprocal Theorem the latter should also be 4.1×10^{-5}. However, if the fetch is increased to $\xi = 10^5$, the concentration profiles for sources at $z_s/z_0 = 10^3$ and $z_s/z_0 = 1$ are very similar and approximately constant from $z/z_0 = 1$ to 10^3. Therefore for $\xi = 10^5$ the Reciprocal Theorem applied to the TS model prediction at $z/z_0 = 10^3$ for a source at z_0 gives a close estimate of the concentration at z_0 due to a source at $z_s/z_0 = 10^3$. At distances $\xi > 10^5$ downwind of a source at $z_s/z_0 = 10^3$, no significant discrepancy between the predictions of the TS model and the Reciprocal Theorem was observed.

Fundamental to the Reciprocal Theorem is the assumption that the turbulent flux may be related to the mean concentration gradient using an eddy diffusivity which is a property of the turbulence alone, $F_z = -K \partial c/\partial z$. This closure scheme is not valid if the concentration gradient may vary significantly over a distance of the order of the length scale of the turbulence (Tennekes and Lumley, 1972; Corrsin, 1974) as it must a short distance downwind of an elevated source. To illustrate this point, Figure 2 shows the concentration profiles a distance $\xi = 10^5$ downwind from the leading edge of a plane source at $z_s/z_0 = (10^3, 10^2, 10^1, 10^0)$. The peaks at the source height predicted by the TS model
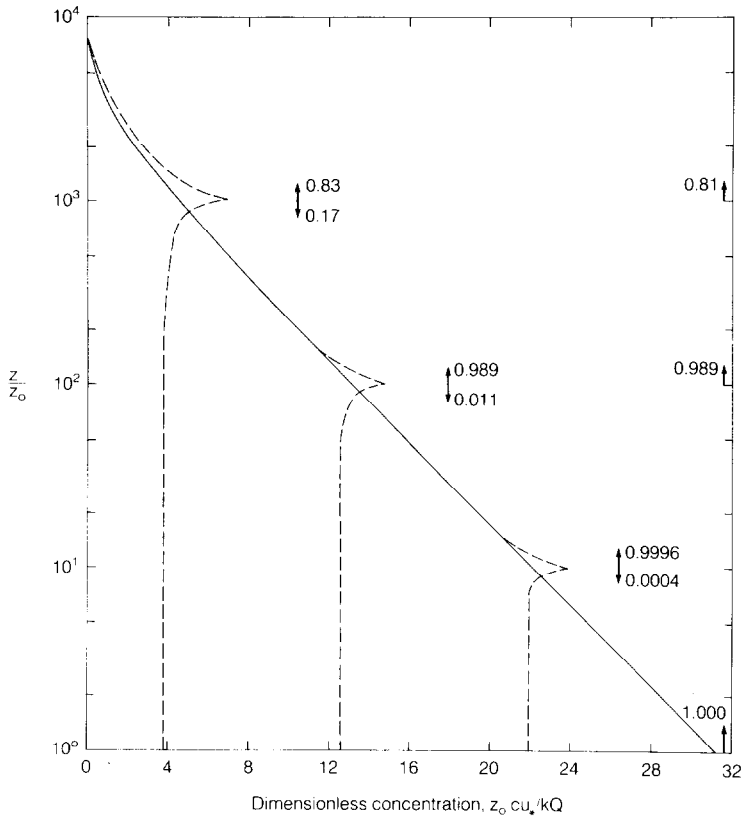
Fig. 2. Dimensionless concentration profile at the downwind edge of a plane source of length $\xi = 10^5$ in the neutral surface layer. Dashed curves, $z_s/z_0 = (10^3, 10^2, 10)$. Solid curve, $z_s/z_0 = 1$. The arrows at the right hand margin give the vertical flux for the source at z_0 (normalized to an emission rate of 1). The arrows at each source height give the upward and downward fluxes at the elevated source. The flux below the elevated source is very small because of the reflecting surface.

are not artificial. They occur because a large proportion of the material seen at the source height has come from immediately upwind and has been travelling for a time which is short compared to the local value of the Lagrangian timescale. According to the statistical theory of Taylor (1921), the effective diffusivity at the source height is therefore smaller than $K_\infty = \sigma_w^2 \tau_L$, and the concentration gradients adjacent to the source are larger than one would expect if $K = K_\infty$.

The Reciprocal Theorem overestimates ground-level concentration due to an elevated source because it overestimates the diffusivity near the source and therefore the rate of transport from the source to the ground. For $\xi = 10^3, 10^4, 10^5, 10^6, 10^7$, and $z_s/z_0 = 10^2$, $10^3, 10^4, 10^5, 10^6$, respectively, the ratios of ground-level concentration due to an elevated line source in the neutral surface layer according to the TS model and according to the Reciprocal Theorem (applied to the TS results for a ground-level source) are 0.72, 0.67, 0.65, 0.62, 0.43. Although the Reciprocal Theorem predicts surface concentrations of correct order of magnitude, the accuracy at given ξ/z_s decreases as source height

increases. One would expect the Reciprocal Theorem to be even less accurate in unstable
stratification, because of the increased length scale at the source height (and vice versa
in stable stratification). For $\xi = 10^4$, $z_s/z_0 = 10^3$, the ratios of concentration according
to the TS model and according to the Reciprocal Theorem are 0.60, 0.67, 0.98 for
$\Omega = -1 \times 10^3$, 0, 1×10^3, respectively.

In summary, at short distances downwind of an elevated source, the Reciprocal
Theorem is invalid, but as the fetch increases, the theorem becomes increasingly (even-
tually perfectly) accurate. There is no reason to believe that this trend would be different
for an elevated source outside the surface layer or at a very long distance from a surface
layer source.

4.2. GROUND-LEVEL SOURCES

Because the length scale of the turbulence becomes very small near the ground, it seems
probable that the flux-mean gradient closure scheme (K-theory) is valid for a ground-level
source. In this case the concentration profile may be obtained by solving the diffusion
equation:

$$u \frac{\partial c}{\partial x} = \frac{\partial}{\partial z}\left(K \frac{\partial c}{\partial z}\right)$$
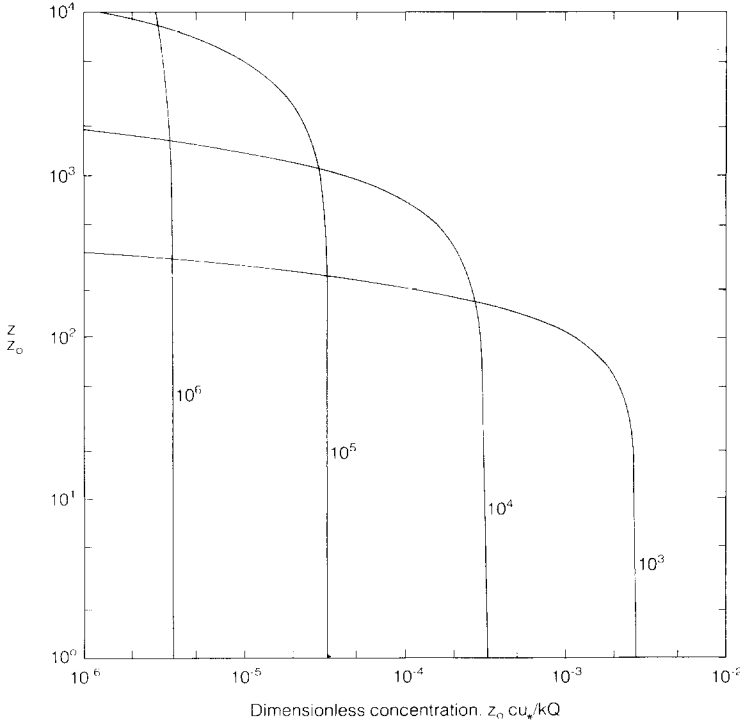
Fig. 3.   Dimensionless concentration profiles at a distance $\xi = (10^3, 10^4, 10^5, 10^6)$ downwind of a line source
at $z_s = z_0$ in the neutral surface layer.

with appropriate $u(z)$, $K(z)$, and boundary conditions. An approximate analytical solution for ground-level line and plane sources in neutral and stable stratification has been obtained and will be reported in a later paper. The analytical solutions for a plane source are very close to the TS model predictions out to a height where concentration drops to $1/10^{th}$ the surface value. For a line source the analytical solutions also agree closely with the TS model at ground and up to a dimensionless height of about $\xi/10^2$. For many purposes the analytical solutions should be adequate, and may be calculated readily. Nevertheless, the predictions of the TS model in stable stratification will be included here because they are believed to be the exact solution at all heights.

Fig. 4.   Dimensionless concentration profile at a distance $\xi = (10^3, 10^4, 10^5, 10^6)$ downwind of the leading edge of a plane source at $z_s = z_0$ in the neutral surface layer.

Figures 3 and 4 give the dimensionless concentration profiles for several values of the distance ξ downwind of a line source at $z_s = z_0$ and downwind of the leading edge of a plane source at $z_s = z_0$ respectively in the neutral surface layer. Figures 5 and 6 give the dimensionless concentration profiles at a distance $\xi = 10^4$ downwind of a line source at $z_s = z_0$ and downwind of the leading edge of a plane source at $z_s = z_0$, respectively, for a range of values of the stability parameter, $-4 \times 10^{-3} \leq \Omega \leq 4 \times 10^{-3}$. Figures 3 and 5 imply that if $\xi \gtrsim 10^4$, for many purposes a knowledge of ground-level concentration alone will be sufficient, because in this case, at least in neutral and unstable stratification, the concentration is approximately constant from ground to $\eta \gtrsim 10^3$ ($z \gtrsim 5$ m for

J. D. WILSON
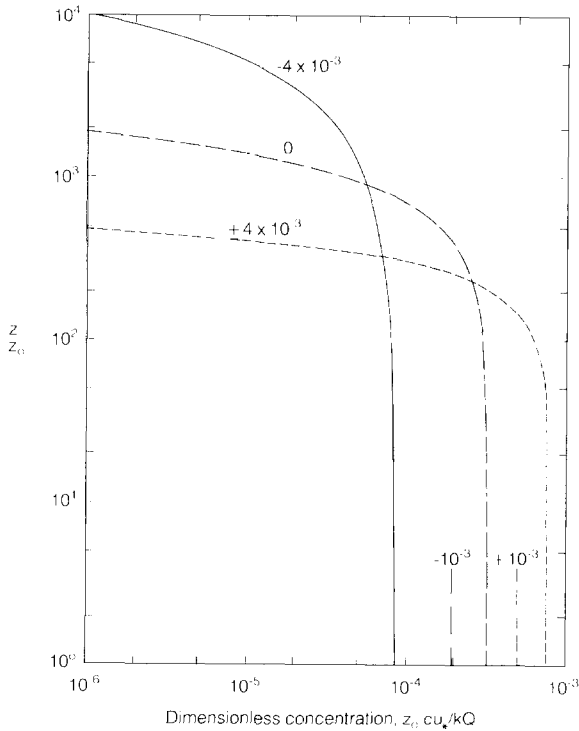
Fig. 5.   Dimensionless concentration profile at a distance $\xi = 10^4$ downwind of a line source at $z_s = z_0$ for
several values of $z_0 L$.

$z_0 = 0.5$ cm). Figure 7 gives the ground-level concentration at distance ξ downwind of
a line source at ground, for several values of Ω. This may be compared with Figure 1
of Horst (1979) and Figure 2 of van Ulden (1978). In neutral stratification the expression
$\chi_0 = 3.2/\xi$ is correct to within about 10% for $10^3 \lesssim \xi \lesssim 10^6$.

The profile for $\xi = 10^3$ in Figure 3 may be compared with that obtained by Yamamoto
and Shimanuki (1961) by numerical integration of the diffusion equation. The two
profiles are similar, but Yamamoto and Shimanuki overestimate the value of $z_0 c u_*/kQ$
at ground-level (4.1×10^{-3} as opposed to 2.8×10^{-3} for the TS estimate) in conse-
quence of having set the mass diffusivity equal to the eddy viscosity. At a longer fetch,
$\xi = 5 \times 10^3$, the solutions given by the numerical integration and the TS model are
respectively 10^{-3} and 6.0×10^{-4}.

Table I gives the dimensionless concentration profiles for a range of distances ξ
downwind of a line source of strength Q at $z_s = z_0$, for $-4 \times 10^{-3} \le \Omega \le 4 \times 10^{-3}$. Note
that $|\Omega| = 4 \times 10^{-3}$ is a fairly large value, corresponding to $z_0 = 2$ cm, $|L| = 500$ cm,
for example. These profiles may also be interpreted as profiles of cross-wind integrated
concentration at an arc of radius ξz_0 centred on a point source of strength Q at $z = z_0$
if u_*/k is derived from the slope of the total horizontal (cup) windspeed.

Table II gives the dimensionless concentration profiles at a range of distances ξ
downwind of the leading edge of a plane source of strength Q at $z_s = z_0$, for

* Therefore $c_0 u_*/kQ \approx 3.2/x$, i.e. concentration is approximately independent of z_0.

Fig. 7. Dimensionless concentration at ground level due to a ground-level line source at a distance ζ upwind, for several values of z_0/L.
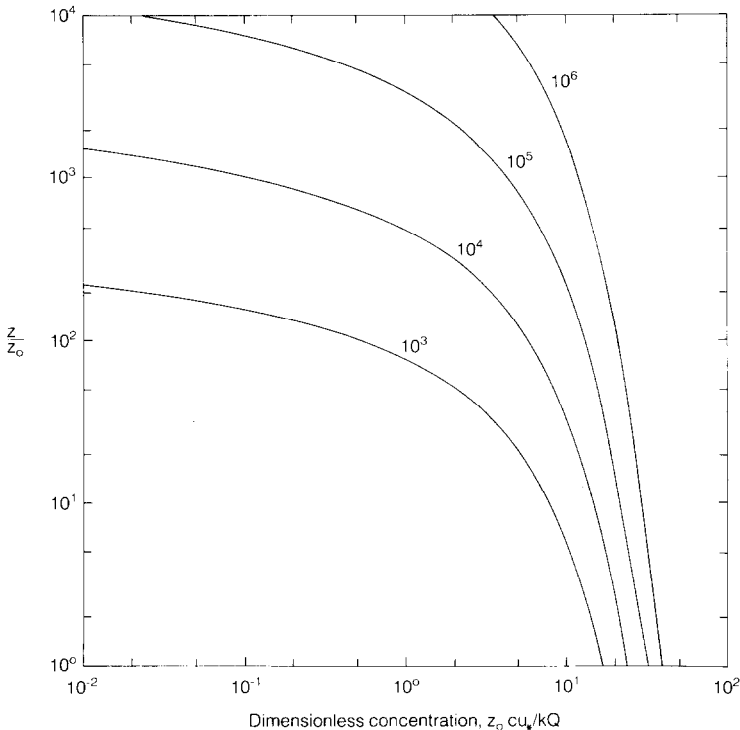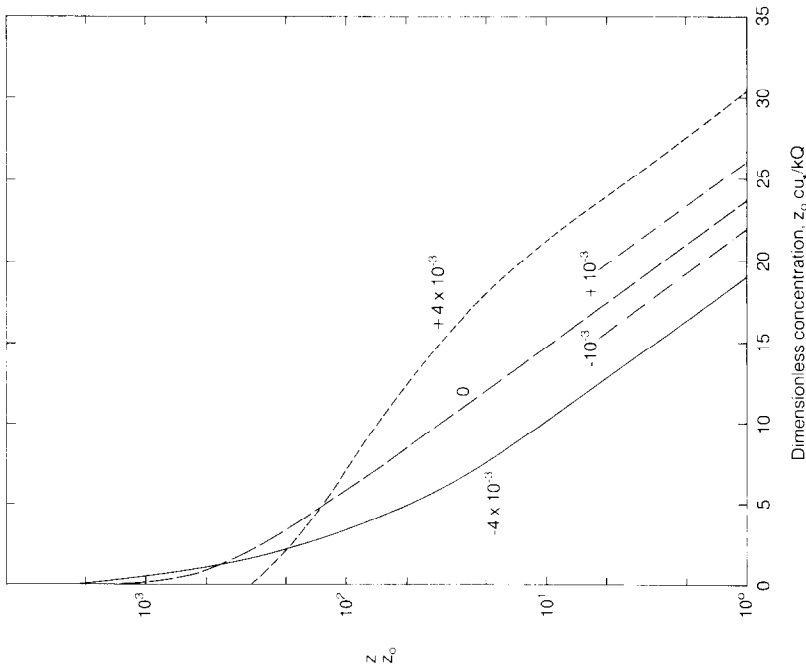

Fig. 6. Dimensionless concentration profile at a distance $\zeta = 10^4$ downwind of the leading edge of a plane source at $z_s = z_0$ for several values of z_0/L.

TABLE I*

Dimensionless concentration profiles $z_0 c u_*/kQ$ downwind of a continuous ground-level line source for several values of ξ, Ω

ξ η	10^3	2×10^3	5×10^3	10^4	2×10^4	5×10^4	10^5	2×10^5	5×10^5	10^6
1	2.8 −3	1.48−3	6.0 −4	3.3 −4	1.67−4	6.9 −5	3.3 −5	1.74−5	7.1 −6	3.6 −6
2	2.8 −3	1.48−3	6.0 −4	3.3 −4	1.67−4	6.9 −5	3.3 −5	1.74−5	7.1 −6	3.6 −6
5	2.8 −3	1.48−3	6.0 −4	3.3 −4	1.67−4	6.9 −5	3.3 −5	1.74−5	7.1 −6	3.6 −6
10	2.7 −3	1.48−3	6.0 −4	3.2 −4	1.66−4	6.9 −5	3.3 −5	1.74−5	7.1 −6	3.6 −6
20	2.7 −3	1.46−3	6.0 −4	3.1 −4	1.60−4	6.9 −5	3.3 −5	1.74−5	7.1 −6	3.6 −6
50	2.2 −3	1.31−3	6.0 −4	3.1 −4	1.59−4	6.8 −5	3.3 −5	1.74−5	7.0 −6	3.6 −6
100	1.20−3	1.02−3	5.5 −4	3.0 −4	1.58−4	6.5 −5	3.3 −5	1.74−5	6.9 −6	3.6 −6
200	1.20−4	4.3 −4	4.1 4	2.6 −4	1.48−4	6.5 −5	3.3 −5	1.73−5	6.9 −6	3.6 −6
500	0	4.5 −6	1.16−4	1.6 −4	1.19−4	6.0 −5	3.2 −5	1.63−5	6.7 −6	3.5 −6
10^3		0	3.8 −6	4.1 −5	7.0 −5	5.0 −5	2.9 −5	1.60−5	6.7 −6	3.5 −6
2×10^3			0	5.7 −7	1.46−5	3.0 −5	2.4 −5	1.51−5	6.7 −6	3.3 −6
5×10^3				0	0	3.2 −6	1.01−5	1.01−5	6.0 −6	3.2 −6
10^4						8.6 −9	1.20−6	3.9 −6	4.6 −6	2.8 −6
2×10^4						0	0	3.5 −7	2.2 −6	2.1 −6
5×10^4								0	7.8 −8	6.0 −7
10^5									0	2.9 −8
	Line, $\Omega = 0$									

ξ	10^3	2×10^3	5×10^3	10^4	2×10^4	5×10^4	10^5
1	2.0 −3	8.0 −4	2.6 −4	8.8 −5	2.7 −5	3.5 −6	9.7 −7
2	2.0 −3	8.0 −4	2.6 −4	8.8 −5	2.7 −5	3.5 −6	9.7 −7
5	1.97−3	8.0 −4	2.6 −4	8.8 −5	2.7 −5	3.5 −6	9.7 −7
10	1.90−3	8.0 −4	2.6 −4	8.8 −5	2.7 −5	3.5 −6	9.7 −7
20	1.86−3	8.0 −4	2.6 −4	8.4 −5	2.6 −5	3.5 −6	9.7 −7
50	1.59−3	7.5 −4	2.3 −4	8.0 −5	2.5 −5	3.5 −6	9.7 −7
100	1.10−3	6.7 −4	2.2 −4	8.0 −5	2.5 −5	3.5 −6	9.7 −7
200	4.7 −4	4.7 −4	2.0 −4	7.5 −5	2.3 −5	3.5 −6	9.7 −7
500	1.71−5	1.40−4	1.39−4	6.3 −5	2.2 −5	3.5 −6	9.7 −7
10^3	1.80−8	1.10−5	8.3 −5	5.4 −5	2.1 −5	3.5 −6	9.7 −7
2×10^3	0	0	2.5 −5	3.8 −5	1.87−5	3.5 −6	9.7 −7
5×10^3			3.9 −7	1.09−5	1.34−5	3.5 −6	9.7 −7
10^4			0	9.9 −7	7.2 −6	3.5 −6	9.7 −7
2×10^4				6.3 −9	1.57−6	3.1 −6	9.7 −7
5×10^4				0	2.6 −8	1.5 −6	9.7 −7
10^5					0	8.1 −7	
	Line, $\Omega = -4 \times 10^{-3}$						

* Because of the approximate inverse relationship between $x_0 c u_*/kQ$ and ξ a precise knowledge of z_0 is not critical for the application of this table.

Table I (continued)

ξ / η	10^3	2×10^3	5×10^3	10^4	2×10^4	5×10^4	10^5
1	2.7 −3	1.39−3	5.0 −4	1.97−4	7.4 −5	1.97−5	5.6 −6
2	2.7 −3	1.35−3	4.9 −4	1.97−4	7.4 −5	1.97−5	5.6 −6
5	2.7 −3	1.30−3	4.7 −4	1.92−4	7.4 −5	1.97−5	5.6 −6
10	2.6 −3	1.25−3	4.6 −4	1.90−4	7.4 −5	1.97−5	5.6 −6
20	2.4 −3	1.19−3	4.6 −4	1.90−4	7.4 −5	1.97−5	5.6 −6
50	2.0 −3	1.14−3	4.3 −4	1.86−4	7.4 −5	1.97−5	5.6 −6
100	1.20−3	8.8 −4	4.0 −4	1.85−4	7.2 −5	1.97−5	5.6 −6
200	2.5 −4	4.7 −4	3.3 −4	1.72−4	7.1 −5	1.85−5	5.6 −6
500	1.8 −7	4.1 −5	1.62−4	1.23−4	6.1 −5	1.63−5	5.3 −6
10^3	0	8.3 −8	3.9 −5	7.2 −5	4.9 −5	1.54−5	5.1 −6
2×10^3		0	1.60−6	2.3 −5	3.1 −5	1.35−5	4.8 −6
5×10^3			0	3.7 −7	8.2 −6	9.9 −6	4.2 −6
10^4				0	6.3 −7	5.7 −6	3.5 −6
2×10^4					6.7 −9	1.9 −6	2.7 −6
5×10^4					0	3.7 −8	9.4 −7
10^5						3.0 −10	1.3 −7

Line, $\Omega = -10^{-3}$

ξ / η	10^3	2×10^3	5×10^3	10^4	2×10^4	5×10^4	10^5
1	2.8 −3	1.48−3	5.3 −4	2.7 −4	1.15−4	3.4 −5	1.34−5
2	2.8 −3	1.48−3	5.3 −4	2.7 −4	1.15−4	3.4 −5	1.34−5
5	2.8 −3	1.48−3	5.3 −4	2.7 −4	1.15−4	3.4 −5	1.34−5
10	2.7 −3	1.41−3	5.3 −4	2.6 −4	1.15−4	3.4 −5	1.34−5
20	2.6 −3	1.38−3	5.3 −4	2.5 −4	1.15−4	3.4 −5	1.34−5
50	2.1 −3	1.22−3	5.2 −4	2.5 −4	1.15−4	3.4 −5	1.34−5
100	1.11−3	9.6 −4	4.8 −4	2.5 −4	1.15−4	3.4 −5	1.16−5
200	1.93−4	4.5 −4	3.8 −4	2.1 −4	1.02−4	3.3 −5	1.12−5
500	0	1.35−5	1.50−4	1.42−4	8.7 −5	3.1 −5	1.07−5
10^3		0	1.59−5	6.2 −5	6.0 −5	2.6 −5	1.03−5
2×10^3			5.5 −8	8.7 −6	3.0 −5	2.1 −5	9.6 −6
5×10^3			0	2.4 −8	2.4 −6	1.11−5	7.5 −6
10^4				0	2.6 −8	3.7 −6	4.9 −6
2×10^4					0	−	2.3 −6
5×10^4							1.7 −7
10^5							1.8 −9

Line, $\Omega = -4 \times 10^{-4}$

Table I (continued)

ξ / η	10^3	2×10^3	5×10^3	10^4	2×10^4	5×10^4	10^5
1	4.0 − 3	2.4 − 3	1.22 − 3	7.4 − 4	4.6 − 4	2.5 − 4	1.54 − 4
2	4.0 − 3	2.4 − 3	1.22 − 3	7.4 − 4	4.6 − 4	2.5 − 4	1.54 − 4
5	4.0 − 3	2.4 − 3	1.22 − 3	7.4 − 4	4.6 − 4	2.5 − 4	1.54 − 4
10	4.0 − 3	2.4 − 3	1.22 − 3	7.4 − 4	4.6 − 4	2.5 − 4	1.54 − 4
20	3.8 − 3	2.3 − 3	1.21 − 3	7.4 − 4	4.6 − 4	2.5 − 4	1.54 − 4
50	2.4 − 3	1.93 − 3	1.10 − 3	7.3 − 4	4.5 − 4	2.5 − 4	1.54 − 4
100	4.4 − 4	8.7 − 4	8.6 − 4	6.2 − 4	4.3 − 4	2.4 − 4	1.52 − 4
200	0	2.4 − 5	2.5 − 4	3.5 − 4	3.2 − 4	2.1 − 4	1.44 − 4
500		0	0	8.5 − 7	2.0 − 5	7.5 − 5	8.2 − 5
10^3				0	0	3.4 − 7	5.5 − 6
2×10^3						0	0

Line, $\Omega = 4 \times 10^{-3}$

ξ / η	10^3	2×10^3	5×10^3	10^4	2×10^4	5×10^4	10^5
1	3.0 − 3	1.78 − 3	8.1 − 4	5.0 − 4	3.0 − 4	1.54 − 4	9.6 − 5
2	3.0 − 3	1.78 − 3	8.1 − 4	5.0 − 4	3.0 − 4	1.54 − 4	9.6 − 5
5	3.0 .− 3	1.78 − 3	8.1 − 4	5.0 − 4	3.0 − 4	1.54 − 4	9.6 − 5
10	3.0 − 3	1.78 − 3	8.1 − 4	4.9 − 4	3.0 − 4	1.54 − 4	9.6 − 5
20	3.0 − 3	1.66 − 3	8.0 − 4	4.9 − 4	3.0 − 4	1.54 − 4	9.6 − 5
50	2.3 − 3	1.57 − 3	7.9 − 4	4.9 − 4	3.0 − 4	1.54 − 4	9.6 − 5
100	1.02 − 3	1.06 − 3	7.1 − 4	4.6 − 4	2.9 − 4	1.54 − 4	9.6 − 5
200	3.7 − 5	2.9 − 4	4.4 − 4	3.6 − 4	2.6 − 4	1.51 − 4	9.3 − 5
500	0	0	1.69 − 5	9.0 − 5	1.30 − 4	1.16 − 4	8.4 − 5
10^3			0	4.5 − 7	1.04 − 5	4.4 − 5	5.2 − 5
2×10^3				0	0	3.1 − 7	5.0 − 6
5×10^3						0	0

Line, $\Omega = 10^{-3}$

ξ / η	10^3	2×10^3	5×10^3	10^4	2×10^4	5×10^4	10^5
1	3.0 − 3	1.64 − 3	7.0 − 4	4.0 − 4	2.3 − 4	1.17 − 4	7.0 − 5
2	3.0 − 3	1.64 − 3	7.0 − 4	4.0 − 4	2.3 − 4	1.17 − 4	7.0 − 5
5	3.0 − 3	1.64 − 3	7.0 − 4	4.0 − 4	2.3 − 4	1.17 − 4	7.0 − 5
10	3.0 − 3	1.64 − 3	7.0 − 4	4.0 − 4	2.3 − 4	1.17 − 4	7.0 − 5
20	2.7 − 3	1.61 − 3	7.0 − 4	4.0 − 4	2.3 − 4	1.17 − 4	7.0 − 5
50	2.2 − 3	1.45 − 3	7.0 − 4	4.0 − 4	2.3 − 4	1.17 − 4	7.0 − 5
100	1.08 − 3	1.03 − 3	6.2 − 4	3.8 − 4	2.3 − 4	1.17 − 4	7.0 − 5
200	6.9 − 5	3.7 − 4	4.4 − 4	3.3 − 4	2.1 − 4	1.15 − 4	6.8 − 5
500	0	0	6.0 − 5	1.37 − 4	1.43 − 4	9.6 − 5	6.5 − 5
10^3			0	9.0 − 6	4.3 − 5	6.2 − 5	5.4 − 5
2×10^3				0	1.37 − 7	9.9 − 6	2.2 − 5
5×10^3					0	0	5.3 − 9
10^4							0

Line, $\Omega = 4 \times 10^{-4}$

TABLE II*

Dimensionless concentration profiles cu_*/kQ and vertical flux profiles F_z/Q (at heights labelled F5, e.t.c.) at the downstream edge of a continuous ground-level plane source for several values of ξ, Ω

ξ η	10^3	2×10^3	5×10^3	10^4	2×10^4	5×10^4	10^5	2×10^5	5×10^5	10^6
1	1.70+1	1.92+1	2.20+1	2.40+1	2.62+1	2.96+1	3.2 +1	3.4 +1	3.7 +1	3.9 +1
2	1.44+1	1.64+1	1.91+1	2.11+1	2.34+1	2.67+1	2.90+1	3.1 +1	3.4 +1	3.6 +1
5	1.05+1	1.26+1	1.53+1	1.75+1	1.96+1	2.30+1	2.51+1	2.75+1	3.0 +1	3.3 +1
F5	0.99	0.99	1.00	1.00	1.00	1.00	1.00	1.00	1.00	1.00
10	7.8	9.8	1.26+1	1.46+1	1.68+1	1.98+1	2.24+1	2.46+1	2.75+1	3.0 +1
20	5.2	7.2	9.9	1.20+1	1.42+1	1.71+1	1.94+1	2.18+1	2.48+1	2.73+1
50	2.18	3.8	6.4	8.5	1.06+1	1.35+1	1.58+1	1.80+1	2.13+1	2.36+1
F50	0.62	0.79	0.91	0.95	0.98	0.99	1.00	1.00	1.00	1.00
100	5.5 −1	1.68	3.8	5.8	7.8	1.09+1	1.32+1	1.55+1	1.86+1	2.10+1
200	2.3 −2	3.5 −1	1.73	3.4	5.3	8.1	1.04+1	1.28+1	1.59+1	1.82+1
500	0	8.6 −4	1.78−1	9.1 −1	2.38	4.8	6.8	9.3	1.23+1	1.47+1
F500	0	0.00	0.11	0.36	0.62	0.83	0.91	0.95	0.98	0.99
10^3		0	2.3 −3	1.12−1	7.1 −1	2.45	4.5	6.6	9.6	1.20+1
2×10^3			0	6.1 −4	6.8 −2	8.6 −1	2.25	4.1	7.0	9.4
5×10^3				0	1.24−6	3.3 −2	4.0 −1	1.48	3.9	5.9
$F5\times10^3$					0.00	0.25	0.25	0.47	0.75	0.87
10^4					0	2.5 −5	2.1 −2	2.8 −1	1.77	3.6
2×10^4						0	0	1.14−2	4.6 −1	1.58
5×10^4								0	6.0 −3	1.84−1
$F5\times10^4$									0.01	0.10

Plane, $\Omega = 0$

ξ η	10^3	2×10^3	5×10^3	10^4	2×10^4	5×10^4	10^5
1	1.60+1	1.70+1	1.84+1	1.95+1	200+1	2.03+1	2.04+1
2	1.31+1	1.44+1	1.55+1	1.64+1	1.70+1	1.73+1	1.74+1
5	9.4	1.06+1	1.21+1	1.28+1	1.32+1	1.36+1	1.37+1
F5	0.99	1.00	1.00	1.00	1.00	1.00	1.00
10	6.9	8.2	9.5	1.02+1	1.07+1	1.10+1	1.11+1
20	4.6	5.8	7.2	7.7	8.2	8.7	8.7
50	2.02	3.1	4.4	5.0	5.5	5.8	5.9
F50	0.75	0.89	0.97	0.99	1.00	1.00	1.00
100	7.8 −1	1.62	2.75	3.4	3.9	4.1	4.2
200	1.64−1	6.4 −1	1.60	2.17	2.62	2.85	3.0
500	1.72−3	8.4 −2	5.8 −1	1.06	1.44	1.36	1.80
F500	0.00	0.15	0.61	0.84	0.95	0.99	1.00
10^3	0	3.0 −3	1.85−1	5.3 −1	8.7 −1	1.13	1.21
2×10^3		4.4 −6	2.95−2	2.09−1	4.7 −1	7.4 −1	8.2 −1
5×10^3		0	2.10−4	2.64−2	1.66−1	3.9 −1	4.7 −1
$F5\times10^3$			0.00	0.11	0.52	0.89	0.98
10^4				1.22−3	4.7 −2	2.15−1	3.1 −1
2×10^4				4.8 −6	5.6 −3	1.05−1	1.92−1
5×10^4				0	5.4 −5	2.0 −2	8.8 −2
$F5\times10^4$					0.00	0.20	0.72
10^5						2.1 −3	3.5 −2
2×10^5						2.3 −4	5.2 −3

Plane, $\Omega = -4 \times 10^{-3}$

* For $\Omega = 0$, $\partial\chi_0/\partial \ln \xi = 3.19$ which implies $(\partial\chi_0/\partial z_0)_x = -3.19/z_0$. Again, high precision in z_0 is not necessary to apply this table.

416

J. D. WILSON

Table II (continued)

ξ η	10^3	2×10^3	5×10^3	10^4	2×10^4	5×10^4	10^5
1	1.67 + 1	1.86 + 1	2.07 + 1	2.21 + 1	2.34 + 1	2.48 + 1	2.50 + 1
2	1.40 + 1	1.58 + 1	1.80 + 1	1.93 + 1	2.06 + 1	2.19 + 1	2.22 + 1
5	1.03 + 1	1.19 + 1	1.42 + 1	1.56 + 1	1.68 + 1	1.80 + 1	1.85 + 1
F5	0.99	0.99	1.00	1.00	1.00	1.00	1.00
10	7.7	9.3	1.15 + 1	1.29 + 1	1.42 + 1	1.53 + 1	1.59 + 1
20	5.0	6.7	8.9	1.03 + 1	1.16 + 1	1.25 + 1	1.31 + 1
50	2.17	3.6	5.6	7.0	8.2	9.3	9.8
F50	0.67	0.82	0.93	0.97	0.99	1.00	1.00
100	6.3 −1	1.68	3.5	4.7	5.9	7.0	7.5
200	6.1 −2	4.8 −1	1.75	2.88	3.9	5.0	5.5
500	0	1.39−2	3.8 −1	1.10	1.96	2.9	3.4
F500	0	0.02	0.30	0.62	0.83	0.96	0.99
10^3		1.5 −5	4.7 −2	3.6 −1	9.7 −1	1.80	2.22
2×10^3		0	7.5 −4	6.2 −2	3.7 −1	1.01	1.41
5×10^3			0	4.3 −4	4.2 −2	3.8 −1	7.0 −1
F5 × 10^3				0.00	0.10	0.59	0.85
10^4				0	1.64−3	1.20−1	3.6 −1
2×10^4					1.1 −5	2.2 −2	1.58−1
5×10^4					0	2.1 −4	2.1 −2
F5 × 10^4						0.00	0.12
10^5							2.0 −3

Plane, $\Omega = -10^{-3}$

ξ η	10^3	2×10^3	5×10^3	10^4	2×10^4	5×10^4	10^5
1	1.67 + 1	1.90 + 1	2.13 + 1	2.31 + 1	2.48 + 1	2.70 + 1	2.78 + 1
2	1.40 + 1	1.60 + 1	1.85 + 1	2.04 + 1	2.21 + 1	2.40 + 1	2.50 + 1
5	1.04 + 1	1.22 + 1	1.48 + 1	1.66 + 1	1.84 + 1	2.01 + 1	2.13 + 1
F5	0.99	0.99	1.00	1.00	1.00	1.00	1.00
10	7.7	9.5	1.21 + 1	1.39 + 1	1.56 + 1	1.75 + 1	1.84 + 1
20	5.2	7.0	9.5	1.12 + 1	1.30 + 1	1.48 + 1	1.57 + 1
50	2.13	3.7	6.0	7.8	9.4	1.12 + 1	1.22 + 1
F50	0.63	0.81	0.92	0.96	0.98	0.99	1.00
100	5.7 −1	1.70	3.7	5.3	7.0	8.7	9.7
200	3.7 −2	3.9 −1	1.75	3.1	4.6	6.4	7.3
500	0	4.3− 3	2.90−1	1.05	2.18	3.7	4.6
F500		0.00	0.20	0.51	0.75	0.92	0.97
10^3		0	1.54−2	2.4 −1	9.0 −1	2.13	2.95
2×10^3			2.5 −5	1.71−2	2.42−1	1.05	1.80
5×10^3			0	1.6 −5	8.4 −3	2.69−1	7.5 −1
F5 × 10^3				0.00	0.02	0.34	0.69
10^4					4.0 −5	4.7 −2	2.8 −1
2×10^4					0	−	7.4 −2
5×10^4							2.3 −3
F5 × 10^4							0.01
10^5							1.1 −5

Plane, $\Omega = -4 \times 10^{-4}$

Table II (continued)

ξ / η	10^3	2×10^3	5×10^3	10^4	2×10^4	5×10^4	10^5
1	1.90 + 1	2.20 + 1	2.69 + 1	3.16 + 1	3.71 + 1	4.7 + 1	5.6 + 1
2	1.61 + 1	1.90 + 1	2.39 + 1	2.86 + 1	3.43 + 1	4.4 + 1	5.3 + 1
5	1.21 + 1	1.50 + 1	2.00 + 1	2.47 + 1	3.06 + 1	3.9 + 1	4.9 + 1
F5	0.98	0.99	0.99	1.00	1.00	1.00	1.00
10	9.1	1.21 + 1	1.70 + 1	2.14 + 1	2.72 + 1	3.7 + 1	4.6 + 1
20	5.9	8.6	1.35 + 1	1.78 + 1	2.38 + 1	3.4 + 1	4.3 + 1
50	1.75	4.0	8.1	1.23 + 1	1.80 + 1	2.75 + 1	3.7 + 1
F50	0.42	0.63	0.76	0.86	0.91	0.96	0.97
100	1.40 − 1	8.7 − 1	3.7	7.2	1.23 + 1	2.15 + 1	3.1 + 1
200	0	9.2 − 3	4.7 − 1	2.04	5.4	1.30 + 1	2.21 + 1
500		0	0	1.32 − 3	9.2 − 2	1.70	5.7
F500				0.00	0.02	0.15	0.36
10^3				0	0	1.40 − 3	1.11 − 1
2×10^3						0	0
	Plane, $\Omega = 4 \times 10^{-3}$						

ξ / η	10^3	2×10^3	5×10^3	10^4	2×10^4	5×10^4	10^5
1	1.76 + 1	2.02 + 1	2.35 + 1	2.67 + 1	3.02 + 1	3.62 + 1	4.24 + 1
2	1.49 + 1	1.74 + 1	2.07 + 1	2.39 + 1	2.75 + 1	3.35 + 1	3.95 + 1
5	1.12 + 1	1.34 + 1	1.69 + 1	2.00 + 1	2.38 + 1	2.99 + 1	3.57 + 1
F5	0.99	0.99	1.00	1.00	1.00	1.00	1.00
10	8.2	1.04 + 1	1.41 + 1	1.70 + 1	2.08 + 1	2.70 + 1	3.29 + 1
20	5.4	7.7	1.13 + 1	1.42 + 1	1.79 + 1	2.41 + 1	3.00 + 1
50	2.10	4.0	7.2	1.01 + 1	1.38 + 1	2.02 + 1	2.61 + 1
F50	0.57	0.74	0.86	0.92	0.95	0.97	0.98
100	4.2 − 1	1.50	4.0	6.9	1.02 + 1	1.65 + 1	2.23 + 1
200	5.7 − 3	1.61 − 1	1.43	3.4	6.5	1.20 + 1	1.79 + 1
500	0	−	1.80 − 2	3.1 − 1	1.53	5.3	1.02 + 1
F500			0.01	0.10	0.28	0.52	0.69
10^3			0	4.1 − 4	4.4 − 2	9.2 − 1	3.4
2×10^3				0	0	2.0 − 3	1.33 − 1
5×10^3						0	0
	Plane, $\Omega = 10^{-3}$						

Table II (continued)

ζ η	10^3	2×10^3	5×10^3	10^4	2×10^4	5×10^4	10^5
1	1.75 + 1	1.96 + 1	2.28 + 1	2.53 + 1	2.79 + 1	3.29 + 1	3.73 + 1
2	1.46 + 1	1.66 + 1	1.99 + 1	2.24 + 1	2.52 + 1	3.01 + 1	3.47 + 1
5	1.08 + 1	1.28 + 1	1.60 + 1	1.86 + 1	2.16 + 1	2.64 + 1	3.06 + 1
F5	0.99	0.99	1.00	1.00	1.00	1.00	1.00
10	8.0	1.02 + 1	1.33 + 1	1.57 + 1	1.87 + 1	2.36 + 1	2.79 + 1
20	5.3	7.4	1.05 + 1	1.30 + 1	1.60 + 1	2.07 + 1	2.51 + 1
50	2.10	3.9	6.9	9.3	1.22 + 1	1.68 + 1	2.12 + 1
F50	0.60	0.76	0.89	0.94	0.96	0.98	0.99
100	4.8 − 1	1.56	4.0	6.4	9.1	1.38 + 1	1.82 + 1
200	1.45 − 2	2.62 − 1	1.60	3.5	6.0	1.05 + 1	1.47 + 1
500	0	–	8.0 − 2	6.3 − 1	2.2	5.7	9.1
F500			0.04	0.21	0.40	0.63	0.80
10^3			0	1.62 − 2	2.9 − 1	2.0	4.9
2×10^3				0	5.8 − 4	1.52 − 1	1.00
5×10^3					0	0	5.3 − 4
F5 × 10³							0.00
	Plane, $\Omega = 4 \times 10^{-4}$						

$-4 \times 10^{-3} \leq \Omega \leq 4 \times 10^3$. Also included are the values of the normalized vertical flux density $F_z(\eta)/Q$. The value of $F_z(\eta)/Q$ may be interpreted as the fraction of the material released from the leading edge of the source which passes ζ above η.

There is a statistical uncertainty in each concentration profile generated by the TS model which decreases in proportion to the reciprocal of the square root of the number of particles (NP) released. In the profiles tabulated here the uncertainty has been reduced to a very low level, but small ($< 5\%$) irregularities may remain.

The nature and depth of the surface layer and the limitations of the TS model must be kept in mind when applying these predictions. For example, the profile for $\zeta = 10^6$ cannot be used for large z_0. If $z_0 = 1$ cm, then $x = 10$ km, and from Table II under neutral stratification 10% of the material from the leading edge passes $\zeta = 10^6$ ($x = 10$ km) above $\eta = 5 \times 10^4$ ($z = 500$ m). However, the surface-layer depth is of the order of 100 m, so that this would be an invalid application of the TS model. Under very stable stratification the surface-layer depth may be only several meters.

The predictions given in Tables I and II may be modified for application to experiments over a short crop only if the displacement height, d, defined by fitting the above-crop neutral wind profile to the equation:

$$u = \frac{u_*}{k} \ln \frac{z - d}{z_0},$$

is sufficiently small that $\sigma_w \tau = 0.5(z - d)$ is a good approximation to the length scale above the crop in neutral conditions. Then if motion below d is ignored, and the source placed at $d + z_0$, the predictions given may be applied directly with z everywhere

interpreted as $(z - d)$, because the replacement of z with $(z - d)$ in all functions has no effect on the outcome of the simulations other than to displace the entire profile of concentration upward by a distance d.

As an example of a practical application of these tables, consider the problem of estimating the rate of emission to the atmosphere of a volatile component of a chemical spray which has been applied to a large field of short vegetation. For this purpose the profile of dimensionless horizontal flux is most useful, and this may be derived from the given tables of cu_*/kQ simply by multiplying by u/u_*, which is a known function of η, Ω. The first step is to measure z_0 to obtain the dimensionless fetch. Then one may simply measure $\bar{u}$ and $\bar{c}$ at a single height, preferably chosen as the height at which $\bar{c}\,\bar{u}/kQ$ is most insensitive to L, and compare the measured $\bar{c}\,\bar{u}$ with the predicted value of $\bar{c}\,\bar{u}/kQ$ to obtain an estimate of Q. Note that this involves the assumptions that Q is independent of position and that $\bar{u}\,\bar{c} = \overline{uc}$.

5. Conclusion

The dimensionless concentration $z_0 cu_*/kQ$ (or cu_*/kQ) due to a continuous line (area) source of passive admixture in the atmospheric surface layer depends only on z/z_0, x/z_0, z_s/z_0 and z_0/L. One important consequence of this fact is that the vertical spread $\sigma_z(x)$ in the Gaussian Plume model may be replaced with $\sigma_\eta(\xi)$ to obtain a universal curve which is independent of z_0. The fundamental stability parameter for surface-layer dispersion is z_0/L.

The trajectory-simulation model has been used to calculate profiles of dimensionless concentration downwind of elevated line and area sources. These profiles do not obey the Reciprocal Theorem, which relates ground-level concentration due to an elevated source to the concentration profile due to a ground-level source. The discrepancy decreases with increasing fetch and is believed to be due to the inadequacy of the flux-mean gradient closure scheme in the case of an elevated source. The TS model profile also shows that the concentration profile due to an elevated source differs only slightly from that due to a ground-level source if $x/z_0 \gtrsim 10^2\, z_s/z_0$.

Dimensionless concentration profiles due to ground-level line and area sources are tabulated for a useful range of x/z_0 and z_0/L. It is hoped that these tables will be of practical use to those involved in surface-layer dispersion problems.

References

Abramowitz, M. and Stegun, I. A.: 1970, *Handbook of Mathematical Functions*, Dover Publications Inc., New York.

Batchelor, G. K.: 1957, 'Diffusion in Free Turbulent Shear Flows', *J. Fluid Mech.* **3**, 67–80.

Cermak, J. E.: 1962, 'Lagrangian Similarity Hypothesis Applied to Diffusion in Turbulent Shear Flow', *J. Fluid Mech.* **15**, 49–64.

Corrsin, S.: 1974, 'Limitations of Gradient Transport Models in Random Walks and in Turbulence', *Adv. Geophys.* **18A**, 25–49.

Gifford, F. A.: 1976, 'Turbulent Diffusion-typing Schemes: A Review', *Nuclear Safety* **17**, 25–43.

Haugen, D. A.: 1973, *Workshop on Micrometeorology*, publication of the American Meteorological Society, Boston, Massachusetts.

Horst, T. W.: 1979, 'Lagrangian Similarity Modelling of Vertical Diffusion from a Ground-Level Source', *J. Appl. Meteorol.* **18**, 733–740.

Pasquill, F.: 1974, *Atmospheric Diffusion*, John Wiley and Sons Inc., New York.

Smith, F. B.: 1957, 'The Diffusion of Smoke from a Continuous Elevated Point-source into a Turbulent Atmosphere', *J. Fluid Mech.* **2**, 49–76.

Taylor, G. I.: 1921, 'Diffusion by Continuous Movements', *Proc. London Math. Soc.* **20**, 196–211.

Tennekes, H. and Lumley, J. L.: 1972, *A First Course in Turbulence*, M.I.T. Press, Cambridge, Massachusetts.

van Ulden, A. P.: 1978, 'Simple Estimates for Vertical Diffusion from Sources near the Ground', *Atmos. Envir.* **12**, 2125–2129.

Wilson, J. D., Thurtell, G. W., and Kidd, G. E.: 1981a, 'Numerical Simulation of Particle Trajectories in Inhomogeneous Turbulence, I: Systems with Constant Turbulent Velocity Scale', *Boundary-Layer Meteorol.* **21**, 295–313.

Wilson, J. D., Thurtell, G. W., and Kidd, G. E.: 1981b, 'Numerical Simulation of Particle Trajectories in Inhomogeneous Turbulence, II: Systems with Variable Turbulent Velocity Scale', *Boundary-Layer Meteorol.* **21**, 423–441.

Wilson, J. D., Thurtell, G. W., and Kidd, G. E.: 1981c, 'Numerical Simulation of Particle Trajectories in Inhomogeneous Turbulence, III: Comparison of Predictions with Experimental Data for the Atmospheric Surface Layer', *Boundary-Layer Meteorol.* **21**, 443–463.

Yamamoto, G. and Shimanuki, A.: 1961, 'Numerical Solution of the Equation of Atmospheric Turbulent Diffusion (1)', *Sci. Reports Tohoku Univ.*, ser. *V*, Geophysics **12**, 24–35.